ACADEMIC PRESS

Available online at www.sciencedirect.com
SCIENCE DIRECT®

Journal of Catalysis 217 (2003) 253–263

JOURNAL OF CATALYSIS

www.elsevier.com/locate/jcat

Sulfur deactivation of NO_x storage catalysts: influence of exposure conditions and noble metal

Annika Amberntsson,[a,b,*] Magnus Skoglundh,[a,c] Sten Ljungström,[a] and Erik Fridell [a,b]

[a] *Competence Centre for Catalysis, Chalmers University of Technology, SE-412 96 Göteborg, Sweden*
[b] *Department of Applied Physics, Chalmers University of Technology, SE-412 96 Göteborg, Sweden*
[c] *Department of Applied Surface Chemistry, Chalmers University of Technology, SE-412 96 Göteborg, Sweden*

Received 26 June 2002; revised 21 November 2002; accepted 6 January 2003

Abstract

In the present study, barium-based NO_x storage catalysts containing platinum, rhodium, or both noble metals were investigated. The influence of SO_2 exposure conditions on the performance of NO_x storage catalysts was studied using flow reactor measurements, FTIR, and XPS where the samples were exposed to lean and/or rich SO_2-containing gas mixtures, simulating the conditions in a mixed lean application. The main results show that all samples are sensitive to sulfur and that deactivation is faster when SO_2 is present in the feed under rich conditions than under lean or continuous SO_2 exposure. It was also found that SO_2 affects the performance of noble metals strongly and that noble metal deactivation most likely occurs during the rich period of a NO_x storage cycle. Additionally, the influence of the noble metals present in the catalysts was investigated with respect to sulfur sensitivity and it was found that a combination of platinum and rhodium seems to be preferable for retaining high performance (high NO oxidation and reduction activity) of the catalyst under SO_2 exposure and subsequent regeneration.

Keywords: Nitrogen oxide; NO_x storage catalyst; NO oxidation; NO reduction; Barium; Sulfur; Platinum; Rhodium

1. Introduction

Increasing environmental concerns have led to a demand for more fuel-effective combustion engines. Lean-burn and diesel engines are interesting for such purposes because of their higher fuel efficiency compared with stoichiometric engines [1]. However, the exhaust from these engines contains a large excess of oxygen, which obstructs reduction of nitrogen oxides (NO_x) to harmless nitrogen in the three-way catalytic converter. One approach to solving this problem is the so-called NO_x storage concept [2–6]. The concept, which is sometimes also referred to as the mixed-lean concept [6] or partial lean strategy [7], is based on adsorption of NO_x during longer periods of oxygen excess followed by shorter periods of oxygen deficit during which the stored NO_x is released and reduced to N_2. Hence, the conditions are substantially varied throughout the cycle. For example, the noble metal surfaces present for oxidation and reduction purposes [8] become, at least partly, oxidized during the lean periods while the metallic forms dominate during the rich periods [9,10]. Additionally, the NO adsorption/desorption behavior of the noble metals will be quite different, as discussed for rhodium single crystals [11] and barium-based NO_x storage catalysts [5,6,12], depending on the surrounding environment. NO-TPD performed with a preoxidized Pt–$Rh/BaO/Al_2O_3$ catalyst releases predominantly NO and O_2 while the desorption products of the prereduced sample are mainly N_2O and N_2 [5,6]. These results agree with single-crystal measurements, and the behavior is explained by suppression of dinitrogen formation in favor of recombination of dissociated NO [11]. The large differences between the rich and lean periods make investigations of the system quite a challenge.

Since the storage of NO_x involves formation of metal nitrates [2–6] the storage compounds usually also show high affinity for sulfate formation [4,13–18]. This frequently results in blockage of the storage sites in the catalyst by the more stable sulfates [17]. Thus, with the fuel sulfur concentration presently at hand (the present European level

* Corresponding author.
E-mail address: ambernt@fy.chalmers.se (A. Amberntsson).

0021-9517/03/$ – see front matter
doi:10.1016/S0021-9517(03)00027-7

of 500 wt-ppm sulfur, S, corresponds to an exhaust gas concentration of about 25 vol-ppm SO_2 [13]) the catalysts need to be regenerated from sulfur on a regular basis. During regeneration, usually reduction at high temperature, the adsorbed sulfur is released as H_2S, COS, and some SO_2 [14,18].

Previous studies have suggested that the poisoning is dependent on accumulated sulfur exposure rather than on SO_2 concentration [13,18]. The exposure temperature, in the working interval of a NO_x storage catalyst, seems to be of minor importance in the deactivation by SO_2 [15]. Formation of sulfates on the catalyst surface and eventually in the bulk material of the catalyst occurs in the presence of oxygen [13,15,16]. FTIR investigations have also shown that formation of sulfates takes place under rich conditions as well [19]. Similar results have been obtained by, among other groups, Matsumoto and co-workers [20], who concluded that doping the conventional barium-on-alumina catalysts with, e.g., titania or zirconia, prevents sulfur poisoning to some extent. Further, these authors also realized that the smaller the sulfate crystals, the easier the decomposition and hence the catalyst regeneration [21,22].

Previously we observed that the deactivation of NO_x storage catalysts is more rapid when the sulfur (SO_2, H_2S, or COS) is present only during the rich phase compared with when it is added only in the lean period [19,23]. It was suggested that this behavior may be related to poisoning of the noble metals or the NO_x storage sites in the vicinity of the noble metal particles.

Previous studies on noble metal-based three-way catalysts have shown that platinum is poisoned by sulfur under rich conditions, possibly by formation of a S layer on the platinum, which can be removed under oxidizing conditions [24,25].

In the present study, the influence of sulfur exposure conditions on the deactivation of a series of three model NO_x storage catalysts with different noble metal compositions was investigated. The catalysts ($Pt/BaO/Al_2O_3$, $Rh/BaO/Al_2O_3$, $Pt–Rh/BaO/Al_2O_3$) were prepared in our laboratory. The effect of adding SO_2 to a synthetic lean-burn exhaust (containing NO, C_3H_6, O_2, and Ar) on the NO_x storage catalyst under either the lean period, the rich period, or continuously during a NO_x storage cycling procedure was studied. The results pointed toward faster deactivation of NO_x storage capacity under rich exposure to SO_2 than when SO_2 was present only during the lean cycle period. Moreover, there were strong indications that these findings can be associated with interactions of sulfur with the noble metals in the samples. The deactivation was found to be less severe when combining platinum and rhodium in the catalysts.

2. Experimental procedure

To simplify and isolate specific characteristics related to sulfur deactivation of NO_x storage catalysts, a number of different model studies were chosen. Hence, the samples prepared included the most essential components of a NO_x storage catalyst, i.e., alumina, barium, and noble metals.

To keep the studied systems simple, the model exhaust contained only propene, nitric oxide, and oxygen during the lean periods, while the rich phases contained propene and nitric oxide. These conditions were chosen even though previous studies had shown that carbon monoxide and hydrogen are the most effective reductants for regeneration of NO_x storage catalysts [26]. For the chosen conditions, we have found that the NO_x storage capacity as well as the NO oxidation and NO reduction functions samples remain at the same levels also after lean–rich cycling for 48 h corresponding to 500 cycles.

To obtain relevant spectroscopic information the noble metal loading was somewhat higher in the samples used for the XPS study. For the FTIR study hydrogen was used as reductant to minimize interference between the spectral features from nitrate and carbonate surface species.

2.1. Catalyst preparation

The preparation route for the monolith catalysts has previously been described in detail [6,27] and is only briefly summarized here. The catalysts prepared are listed in Table 1.

Cordierite substrates (cylindrical, $\phi = 20$ mm, $L = 15$ mm, 400 cells per square inch) were first coated with 500 mg γ-alumina and subsequently with 75 mg barium oxide (derived from $Ba(NO_3)_2$ from Aldrich). The washcoat was deposited by first immersing the substrate into an aqueous slurry of 80 wt% γ-Al_2O_3 (Puralox, Condea) and 20 wt% boehmite (Disperal, Condea). The excess slurry was gently removed by blowing air through the monolith channels. After removal of excess slurry the samples were dried and subsequently calcined. The coating procedure was repeated until the desired amount of alumina was deposited and the samples were then calcined for 90 min at 600 °C in air. The barium oxide was deposited in a similar way using an aqueous solution of barium nitrate. The washcoat composition corresponds to 15 wt% BaO and 85 wt% Al_2O_3 (0.49 and 4.9 mmol, respectively).

Table 1
Catalysts.[a] Overview of studied catalysts

Sample	Type	Pt content (wt%)	Rh content (wt%)
3 wt% $Pt/BaO/Al_2O_3$	Monolith[b]	3	–
2 wt% $Pt/BaO/Al_2O_3$	Monolith	2	–
3 wt% Pt–1.5 wt% $Rh/BaO/Al_2O_3$	Monolith[b]	3	1.5
2 wt% Pt–1 wt% $Rh/BaO/Al_2O_3$	Monolith	2	1
1 wt% $Rh/BaO/Al_2O_3$	Monolith	–	1
2 wt% $Pt/BaO/Al_2O_3$	Powder[c]	2	–

[a] All washcoated samples contained 15 wt% BaO on γ-alumina. Powder samples contained 20 wt% BaO on γ-alumina.
[b] For XPS.
[c] For FTIR.

After washcoating, the samples were impregnated with solutions of the nonhalide platinum and/or rhodium salts ($Pt(NO_3)_2$ from Hereaus and $Pt(NH_3)_4(OH)_2$ and $Rh(NO_3)_2$ from Johnson Matthey), and before use, all catalysts were calcined at 600 °C for 90 min and reduced at 500 °C for 30 min.

For the FTIR measurements powder samples of $Pt/BaO/Al_2O_3$ were prepared using the same preparation procedure as described previously [6] and the same starting materials as for the monolith samples.

2.2. Flow reactor experiments

Each monolith sample was placed in a quartz tube flow reactor system, described elsewhere [28], containing mass flow controllers, temperature control, and instruments for measuring the concentrations of NO, NO_2 (chemiluminescence), and N_2O (IR). The experiments were performed by exposing the samples to synthetic gas mixtures, simulating NO_x storage/release cycles in a mixed lean application [2–6]. The (net oxidizing) adsorption mode was performed in a mixture of 8 vol% O_2, 400 vol-ppm NO, and 500 vol-ppm C_3H_6 balanced with Ar (total flow 3000 ml/min). The temperature was 400 °C, which is close to the maximum in NO_x storage observed for this type of catalyst [6,29]. The equilibrium ratio between NO and NO_2 is close to 1 for 400 vol-ppm NO in 8 vol% O_2 at 400 °C. The adsorption time was 5 min, which was sufficient to saturate the NO_x storage capacity of the samples. The NO_x storage capacity results below are presented in relation to the initial value for each monolith as a function of the S dose or as a function of time. The rich excursions were performed by switching off the oxygen flow and compensating with Ar to maintain constant flow for another 5 min. This is not a realistic time for the rich periods in an engine application, but since the objective of the study was to investigate the influence of sulfur exposure conditions, equally long periods were used for storage and reduction.

2.2.1. Pretreatment

The samples were pretreated by reduction in 2 vol% H_2 at 500 °C for 30 min, oxidation in 10 vol% O_2 at 400 °C for another 30 min, and exposure to 15 sulfur-containing cycles (400 vol-ppm NO, 500 vol-ppm C_3H_6, 25 vol-ppm SO_2, and 0 or 8 vol% O_2 in 5-min-long rich and lean periods, respectively), followed by reduction at 750 °C in 2 vol% H_2 for 30 min and repetition of the oxidation step. The final reduction and oxidation step was performed to provide a stable starting material and to remove adsorbed sulfur species.

2.2.2. Sulfur exposure

The influence of sulfur on NO_x storage performance was studied by adding 25 vol-ppm SO_2 to the gas mixture during the lean, rich, or both periods. The total gas flow was 3000 ml/min, which corresponds to a space velocity of 38,000 h^{-1}. Each experiment contained three sulfur-free (to be used as references) and 15 sulfur-containing storage/regeneration cycles. During the cycles, the NO, NO_2, N_2O, and total NO_x traces were recorded. From these traces the NO_x storage, NO oxidation (lean phase), and NO reduction (rich phase) capacities were evaluated as function of sulfur exposure. Each 5-min period supplied in total 15 μmol of sulfur and 244 μmol of nitrogen oxide. The relative NO oxidation activity for each cycle was calculated as the $[1 - (NO_{out}/NO_{in})] \times 100$ after 4.5 min for each lean SO_2 exposure. The corresponding NO reduction activity for each cycle was calculated as $[(NO_{in} - NO_{out})/NO_{in}] \times 100$ after 4.5 min of rich SO_2 exposure.

2.2.3. Regeneration from sulfur

To investigate the influence of the noble metal composition on the sulfur regenerability of the samples, the deactivated catalysts were reduced in 2 vol% H_2 at 750 °C for 30 min and subsequently exposed to sulfur-free lean–rich NO_x cycles as described above.

2.3. Characterization

2.3.1. XPS

XPS analysis was performed using a Perkin–Elmer PHI 5000C system equipped with a pretreatment cell allowing the samples to be exposed to various gas mixtures and to be transferred between the pretreatment cell and the UHV chamber without being exposed to air. The analysis was performed on small pieces of 3 wt% $Pt/BaO/Al_2O_3$ and 3 wt% Pt–1.5 wt% $Rh/BaO/Al_2O_3$ samples after different pretreatments.

The samples were initially reduced in 8 vol% H_2 at 500 °C for 30 min and then oxidized in 19 vol% O_2 at 400 °C for another 30 min. This pretreatment was chosen to be as similar as possible to the pretreatment used in the flow reactor experiments. After the pretreatment the samples were exposed to either a lean or a rich SO_2-containing gas mixture. The lean gas mixture contained 8 vol% O_2, 400 vol-ppm NO, 500 vol-ppm C_3H_6, and 25 vol-ppm SO_2. The rich mixture had the same composition but with oxygen excluded. The exposure temperature was 400 °C.

The total sulfur exposure time (4 h) and SO_2 flow (total flow approximately 30 ml/min) correspond to an exposure for 20 min with 3000 ml/min in the flow reactor since the sample pieces were approximately 1/10th the size of the corresponding monolith samples used in the flow reactor study. This was expected to result in about 50% loss of NO_x storage capacity under lean exposure and 80% loss for rich exposure (see below).

After SO_2 treatment the samples were reduced in 8 vol% H_2 at 550 °C for 30 min. This procedure was repeated twice.

XPS spectra were recorded after prereduction, sulfur treatment, and both postreductions. The XPS spectra were recorded using non-monochromatic Al-K_α radiation and the Pt $4f$, Rh $3p_{3/2}$, S $2p$, and Al $2s$ levels were studied. The

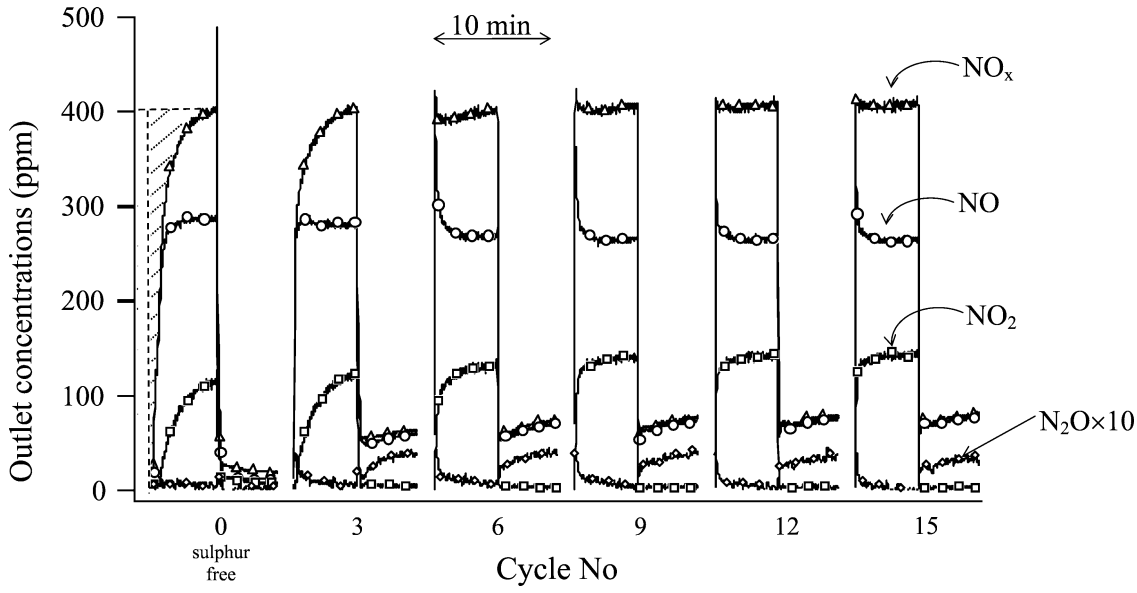

Fig. 1. NO, NO_2, total NO_x and N_2O traces for selected lean/rich cycles when a 2 wt% Pt–1 wt% $Rh/BaO/Al_2O_3$ sample is continuously exposed to 25 vol-ppm SO_2 at 400 °C. Lean gas mixture: 8 vol% O_2, 400 vol-ppm NO, 500 vol-ppm C_3H_6. Rich gas mixture: 400 vol-ppm NO, 500 vol-ppm C_3H_6. Lean time: 5 min. Rich time: 5 min.

energy scale was calibrated by adjusting the Al 2*s* peak to 119.3 eV [30].

2.3.2. FTIR

Characterization of CO on Pt was studied by in situ FTIR experiments in diffuse reflectance (DRIFT) mode with a Bio-Rad FTS6000 spectrometer equipped with a Harrick Praying Mantis DRIFT cell. The powder sample was initially oxidized in 10 vol% O_2 at 500 °C for 15 min and then reduced in 10 vol% H_2 at 500 °C for 15 min. A background spectrum was then taken at 50 °C for the reduced sample. The sample was then exposed to 2 vol% CO until the area of the adsorption band at about 2050 cm^{-1} was constant. The sample was then oxidized and reduced as described above, and exposed to a mixture of 100 vol-ppm SO_2, 1000 vol-ppm NO, and 2 vol% H_2 in Ar at 400 °C for 10 min. After a slight reduction ($\sim$ 5 min in 2 vol% H_2) the sample was cooled to 50 °C and again exposed to 2 vol% CO until saturation.

3. Results

Fig. 1 shows the NO, NO_2, total NO_x ($NO + NO_2$), and N_2O (enhanced by a factor of 10) traces for every third lean/rich cycle in an experiment with continuous SO_2 exposure performed with a 2 wt% Pt–1 wt% Rh/13 wt% BaO/84 wt% Al_2O_3 sample (abbreviated Pt–$Rh/BaO/Al_2O_3$ below). The six cycles shown were measured after exposure to SO_2 doses of 0 (sulfur-free reference), 61, 152, 244, 335, and 427 μmol, respectively. The figure displays the same characteristics as previously discussed by Engström et al. [13]:

i. The NO_x storage capacity of the sample decreases with time, as indicated by the NO_x trace, which assumes a more square-like shape during lean periods as SO_2 exposure is increased.
ii. The NO_x signal during the rich periods increases with exposure time, indicating loss of reduction activity of the noble metals.
iii. N_2O formation during the rich excursions increases with SO_2 exposure time, which also may indicate deactivation of the reduction function of the noble metals.

Two different types of NO breakthrough peaks are observed in Fig. 1. The first type occurs when switching from lean to rich conditions. This peak decreases rapidly with increasing SO_2 exposure. The second type occurs when switching from rich to lean phase. This peak appears after a short period of sulfur exposure and remains.

When the corresponding curves for the experiments with SO_2 present only in either the lean or the rich period are compared (displayed in Fig. 2), the above-mentioned features are observed for both cases. However, under lean SO_2 exposure the breakthrough peak occurring when the conditions are switched from lean to rich disappears significantly faster than under rich sulfur treatment. The opposite behavior is observed when the oxygen is turned back on: the NO_x overshoot in the beginning of the lean period develops much more rapidly when the SO_2 is present during the rich period. Another observation is that the NO_x reduction during the rich period is more affected when the catalyst is subjected to sulfur under the oxygen deficit period.

If the amount of stored NO_x for each cycle in the above-described experiments is calculated as the shadowed area in

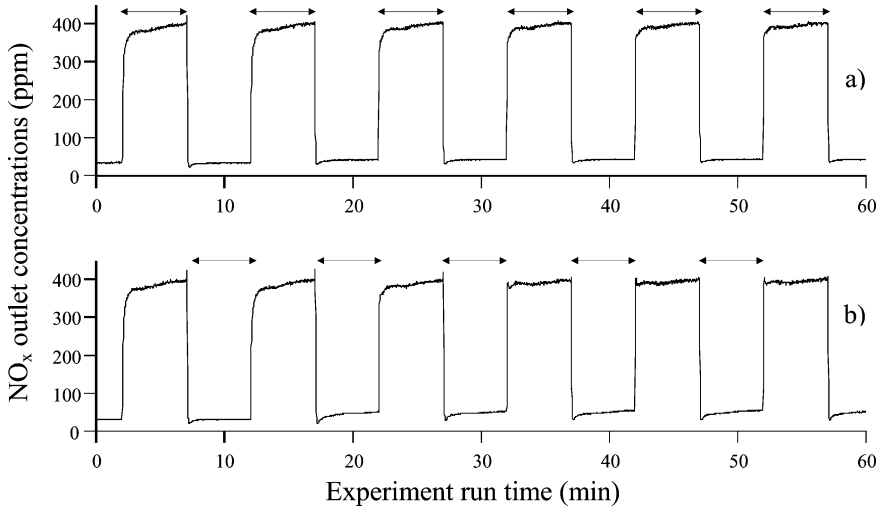

Fig. 2. Outlet traces of NO_x when a 2 wt% Pt–1 wt% $Rh/BaO/Al_2O_3$ sample is exposed to 25 vol-ppm SO_2 at 400 °C under either (a) the lean or (b) the rich cycle period. The arrows indicate where SO_2 is present in the gas mixture. Lean gas mixture: 8 vol% O_2, 400 vol-ppm NO, 500 vol-ppm C_3H_6. Rich gas mixture: 400 vol-ppm NO, 500 vol-ppm C_3H_6. Lean time: 5 min. Rich time: 5 min.

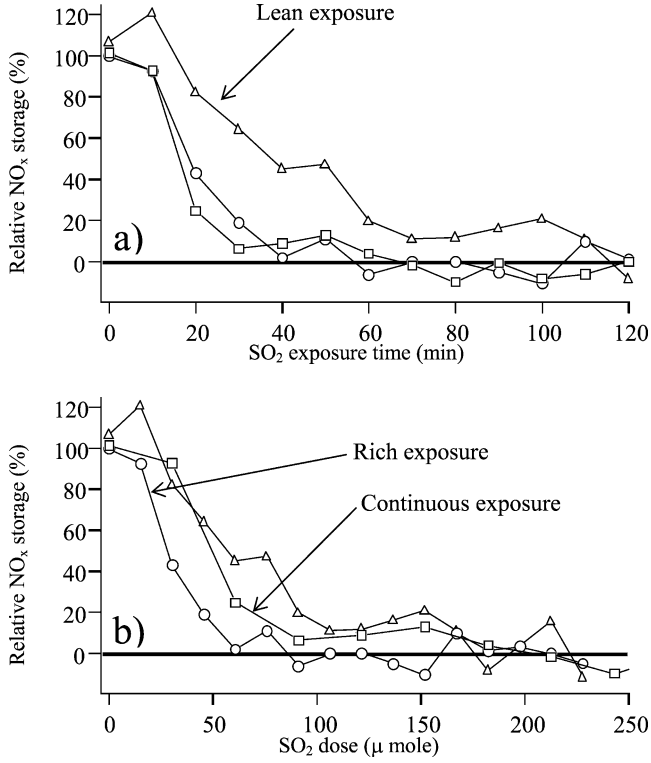

Fig. 3. Normalized NO_x storage capacity during lean (△), rich (○), or continuous (□) exposure to 25 vol-ppm SO_2 at 400 °C of 2 wt% Pt–1 wt% $Rh/BaO/Al_2O_3$ as function of (a) SO_2 exposure time and (b) SO_2 exposure dose. Lean gas mixture: 8 vol% O_2, 400 vol-ppm NO, 500 vol-ppm C_3H_6. Rich gas mixture: 400 vol-ppm NO, 500 vol-ppm C_3H_6. Lean time: 5 min. Rich time: 5 min.

Fig. 1 [6], normalized to the initial value (corresponding to the value received for the initial, sulfur-free cycle in Fig. 1) and plotted versus the SO_2 exposure time or SO_2 exposure dose (see Fig. 3) the NO_x storage deactivation rate under the different exposure conditions can be evaluated. Fig. 3a displays the sulfur deactivation as a function of exposure time. The figure shows that under lean sulfur exposure of Pt–$Rh/BaO/Al_2O_3$, the NO_x storage capacity declines by 50% after about 40 min and complete deactivation is not observed in less than about an hour on stream. The corresponding values for the rich SO_2 treatment experiment are about 20 and 40 min, respectively. Hence, the deactivation rate is significantly higher under rich sulfur exposure than under lean exposure. Fig. 3a also shows that the continuous exposure procedure affects the catalyst in a similar way as the rich exposure when displayed versus time. Note that in the continuous case, twice the amount of SO_2 is supplied per time unit. If the same results are instead plotted versus supplied SO_2 dose (see Fig. 3b), the continuous exposure ends up at an intermediate deactivation rate compared with the lean and rich exposures. Still, the rich exposure procedure results in the most severe deactivation, where the sample is completely deactivated at half the dosage of the lean exposure and two-thirds of the dosage of continuous exposure. In both Figs. 3a and b, the values fluctuate at lower NO_x storage values. This is due to the small amount of NO_x stored and small variations will seem large after normalization.

In Fig. 4 the results of lean (a) and rich (b) SO_2 exposure of Pt–$Rh/BaO/Al_2O_3$ are compared with the corresponding results for the 2 wt% Pt/13 wt% BaO/85 wt% Al_2O_3 catalyst (abbreviated $Pt/BaO/Al_2O_3$ below). The figure shows that behavior similar to that described in Fig. 3 for Pt–$Rh/BaO/Al_2O_3$ is also apparent for $Pt/BaO/Al_2O_3$; the SO_2-rich exposure causes more rapid deactivation than the lean exposure. Additionally, it is evident that the deactivation under lean conditions is almost identical in rate for the different samples. However, during the rich sulfur treatment, the deactivation rate differs between the catalysts and the $Pt/BaO/Al_2O_3$ sample is deactivated considerably faster than the Pt–$Rh/BaO/Al_2O_3$ catalyst. The $Pt/BaO/Al_2O_3$ sample has lost 50% of NO_x storage capacity after 10 min

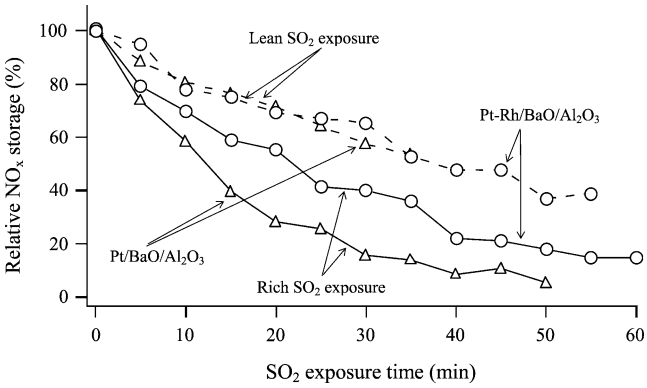

Fig. 4. Normalized NO_x storage capacity during lean (dashed line) or rich (solid line) exposure to 25 vol-ppm SO_2 at 400 °C of 2 wt% Pt/BaO/Al_2O_3 (△) and 2 wt% Pt–1 wt% Rh/BaO/Al_2O_3 (○) as a function of SO_2 exposure time. Lean gas mixture: 8 vol% O_2, 400 vol-ppm NO, 500 vol-ppm C_3H_6. Rich gas mixture: 400 vol-ppm NO, 500 vol-ppm C_3H_6. Lean time: 5 min. Rich time: 5 min.

rich SO_2 exposure while the corresponding capacity of the Pt–Rh/BaO/Al_2O_3 sample exceeds 50% of the initial NO_x storage capacity after 20 min rich sulfur treatment.

In Fig. 5 are shown the NO traces for (a) the lean and (b) rich SO_2 exposure experiments with Pt–Rh/BaO/Al_2O_3. Several features are revealed in this figure. First, the NO signal assumes the shape of a square pulse with increasing SO_2 exposure under both lean and rich SO_2 exposure. Together with the traces displayed in Fig. 2 it is obvious that NO_x storage ability decreases with increasing sulfur dose. The decrease is faster under rich exposure than under lean, as discussed above (see also Fig. 3).

As discussed in Fig. 2, breakthrough peaks occur at the switch between lean and rich conditions. Fig. 5 clearly shows that these peaks originate from NO and that they are effected in opposite ways: SO_2 in the lean period seems to have a suppressing effect on occurrence of the peak when switching from lean to rich, and SO_2 in the rich period seems to have an enhancing effect on occurrence of the peak when switching from rich to lean composition.

The XPS spectra of (a) S $2p$, (b) Pt $4f$, and (c) Rh $3p_{3/2}$ for Pt–Rh/BaO/Al_2O_3 recorded after lean and rich SO_2 exposures are displayed in Fig. 6. The first spectrum (Fig. 6a) shows that under rich exposure the amount of sulfur accumulated in the samples is very low compared with lean exposure. Under both exposure conditions the sulfur is accumulated as sulfate (S $2p$ peak positioned at 169 eV [31]), which is in agreement with Engström et al. [13].

The Pt $4f$ spectra (Fig. 6b) show peak maxima at 71.5 and 74.9 eV after rich exposure and 74.3 eV with shoulders at 71.8 and 77.0 eV after lean SO_2 exposure. These peaks are dominated by metallic platinum (Pt $4f_{7/2}$ occurs at 71 eV and Pt $4f_{5/2}$ occurs at 74 eV for Pt^0 [31]) for the rich SO_2 treatment and probably to a mixture of Pt^0 and platinum oxides (the Pt $4f_{7/2}$ peaks for PtO and PtO_2 are located around 73 and 75 eV, respectively [31,32]) for the lean SO_2 treatment.

The third pair of spectra, shown in Fig. 6c, indicates that Rh is also affected by the different treatments. The rhodium signal is much more intense after lean than after rich SO_2 treatment. This may be associated with enrichment of rhodium at the surface in an oxidative atmosphere [17,33]. A second observation is that the Rh $3p_{3/2}$ peak at 497 eV, observed following rich sulfur treatment, corresponds to metallic rhodium. After lean treatment, on the other hand, the Rh $3p_{3/2}$ peak, is observed 498 eV. For Rh $3d_{5/2}$ a shift from 307 to 308 eV has previously been correlated to Rh_2O_3 formation [31]. In Fig. 6c an upward shift of about 1 eV is observed for the $3p_{3/2}$ peak, making formation of Rh_2O_3 a reasonable assumption. However, it should be noted that $Pt(SO_4)_2$ and $Rh_2(SO_4)_3$ have been reported to be formed after SO_2 and O_2 treatment [34] and most Rh^{3+} species

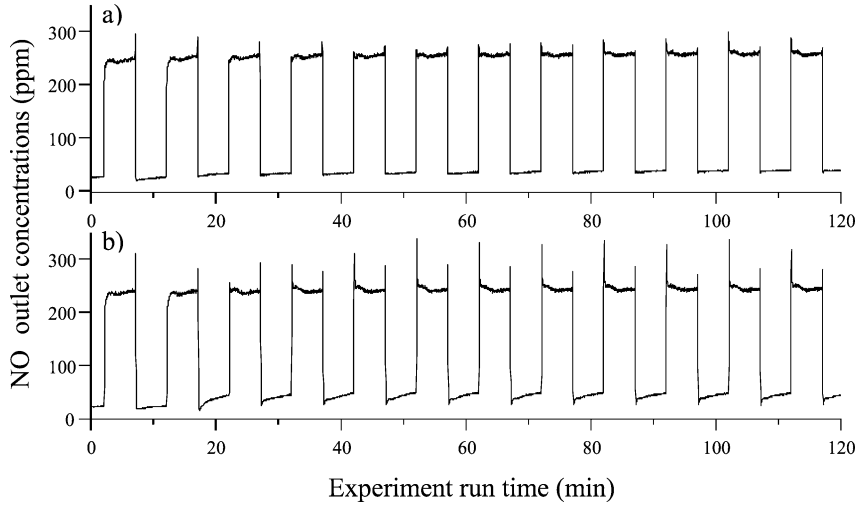

Fig. 5. Outlet traces of NO (a) in the presence of 25 vol-ppm SO_2 during the lean period only (8 vol% O_2, 500 vol-ppm C_3H_6, 400 vol-ppm NO) and (b) in the presence of 25 vol-ppm SO_2 during the rich period only (500 vol-ppm C_3H_6, 400 vol-ppm NO) at 400 °C of a 2 wt% Pt–1 wt% Rh/BaO/Al_2O_3 sample. Lean time: 5 min. Rich time: 5 min.

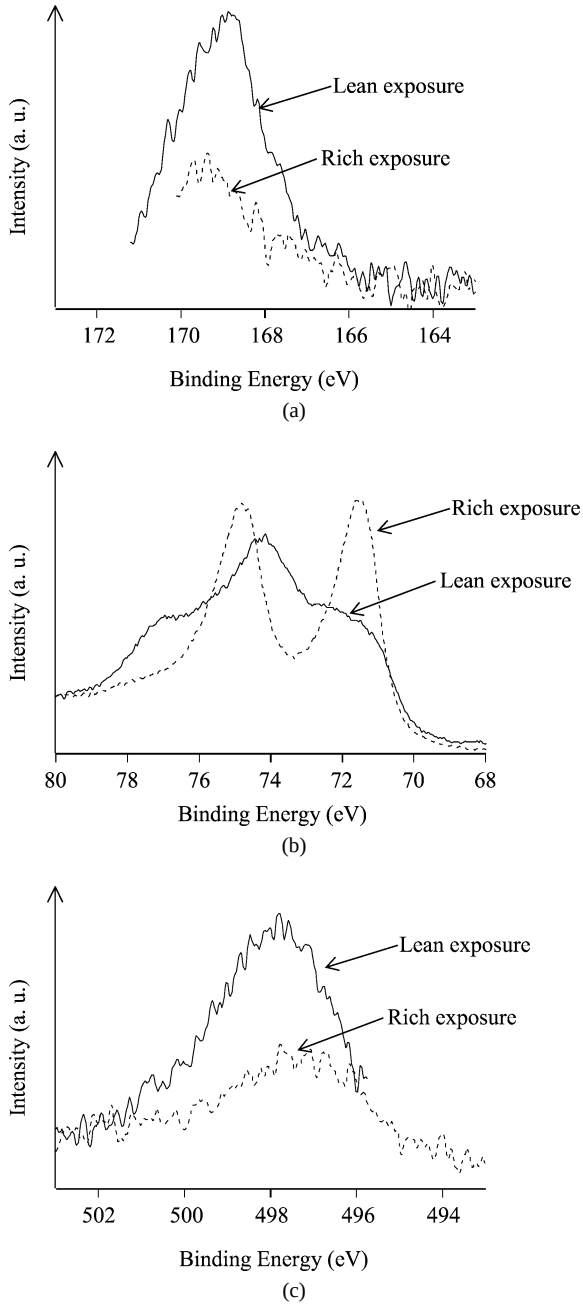

Fig. 6. XPS spectra of (a) S $2p$, (b) Pt $4f$, and (c) Rh $3p_{3/2}$ after rich (solid line) and lean (dashed line) SO_2 exposure of a 3 wt% Pt–1.5 wt% $Rh/BaO/Al_2O_3$ sample. Rich SO_2 treatment: 25 vol-ppm SO_2, 400 vol-ppm NO, and 500 vol-ppm C_3H_6 for 4 h at 400 °C. Lean SO_2 treatment: 8 vol% O_2, 25 vol-ppm SO_2, 400 vol-ppm NO, and 500 vol-ppm C_3H_6 for 4 h at 400 °C.

show Rh $3d_{5/2}$ peaks close to 308 eV [31], making certain assignments difficult.

Fig. 7 shows the IR absorption of CO on platinum in a $Pt/BaO/Al_2O_3$ powder sample before and after rich SO_2 treatment. From the figure it is obvious that the CO chemisorption on the noble metal is drastically decreased when the sample has been exposed to SO_2 under rich conditions.

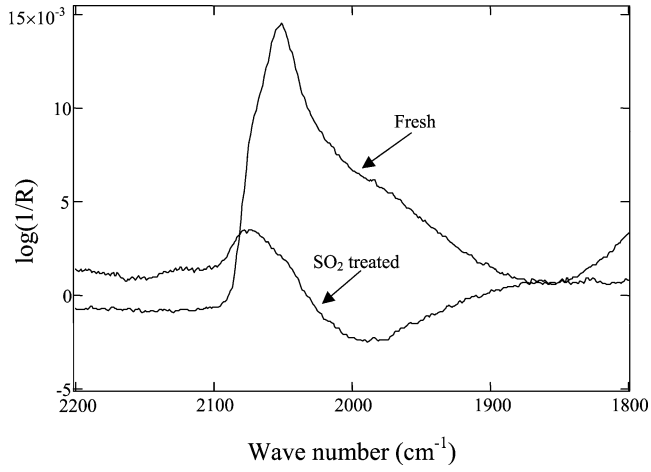

Fig. 7. Chemisorbed CO on 2 wt% Pt of fresh (oxidized in 10 vol% O_2 for 15 min followed by reduction in 10 vol% H_2 for 15 min at 500 °C) and SO_2-treated (100 vol-ppm SO_2, 1000 vol-ppm NO, and 2 vol% H_2 in Ar at 400 °C for 10 min) 2 wt% $Pt/BaO/Al_2O_3$ powder catalyst detected by FTIR.

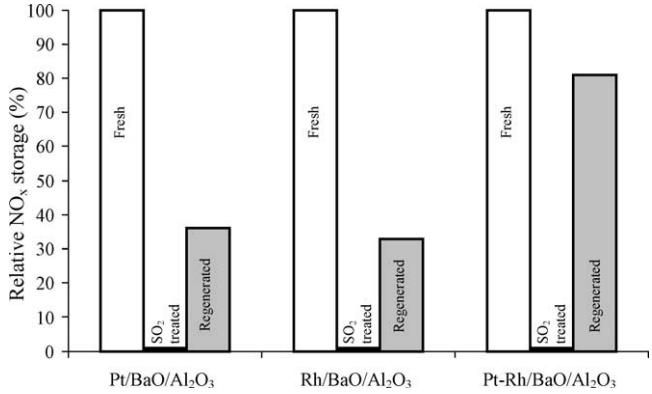

Fig. 8. NO_x storage capacity normalized to initial value for fresh, sulfur-treated, and regenerated 2 wt% $Pt/BaO/Al_2O_3$, 1 wt% $Rh/BaO/Al_2O_3$, and 2 wt% Pt–1 wt% $Rh/BaO/Al_2O_3$. Sulfur exposure procedure: 15 lean/rich cycles in 8 vol% (lean, 5 min) or 0 vol% (rich, 5 min) O_2, 400 vol-ppm NO, 500 vol-ppm C_3H_6, and 25 vol-ppm SO_2 at 400 °C. Regeneration procedure: 2 vol% H_2 at 750 °C for 30 min.

Fig. 8 gives the NO_x storage capacities for $Pt/BaO/Al_2O_3$, $Rh/BaO/Al_2O_3$, and $Pt–Rh/BaO/Al_2O_3$ before and after sulfur treatment, and after sulfur regeneration normalized to the fresh state. The figure indicates that all samples are completely deactivated after the SO_2 exposure and that the NO_x storage ability is recovered after the regeneration procedure. The regeneration does not restore the full initial NO_x storage capacity in any case and from the figure it is clear that the samples containing either platinum or rhodium only regain about 30% of the initial NO_x storage capacity. However, the sample including both noble metals shows much higher regenerability and recovers about 80% of the initial value.

This regenerability is studied in Fig. 9, which shows XPS S $2p$ spectra recorded for fresh, SO_2-treated, and hydrogen-regenerated $Pt/BaO/Al_2O_3$ and $Pt–Rh/BaO/Al_2O_3$ samples. The figure again shows that large amounts of sulfates

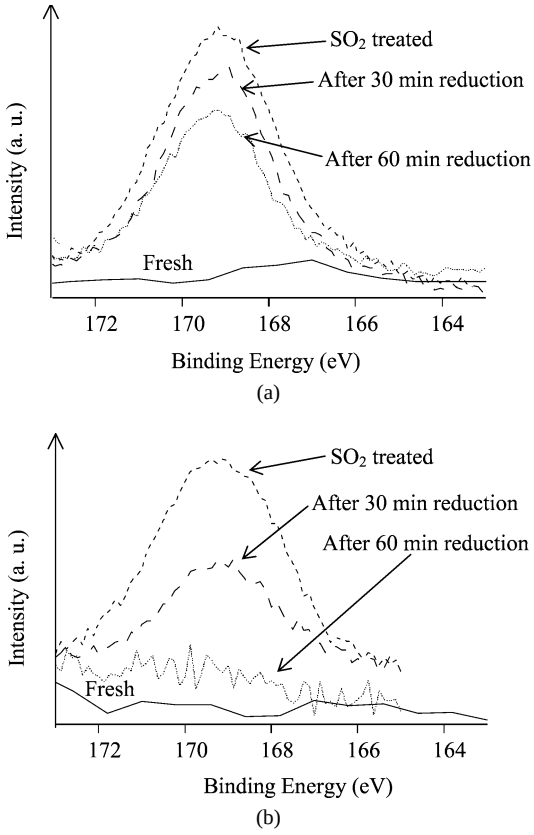

Fig. 9. XPS S 2*p* spectra of (a) 3 wt% $Pt/BaO/Al_2O_3$ and (b) 3 wt% Pt–1.5 wt% $Rh/BaO/Al_2O_3$ after prereduction, i.e., fresh (solid line), SO_2 treatment (small-dashed line), regeneration for 30 min (dashed line), and additional 30 min regeneration (dotted line). Prereduction was performed in 8 vol% H_2 for 30 min at 500 °C. SO_2 treatment was performed in 400 vol-ppm NO, 500 vol-ppm C_3H_6, and 25 vol-ppm SO_2 for 4 h at 400 °C and regenerations were performed in 8 vol% H_2 for 30 + 30 min at 550 °C.

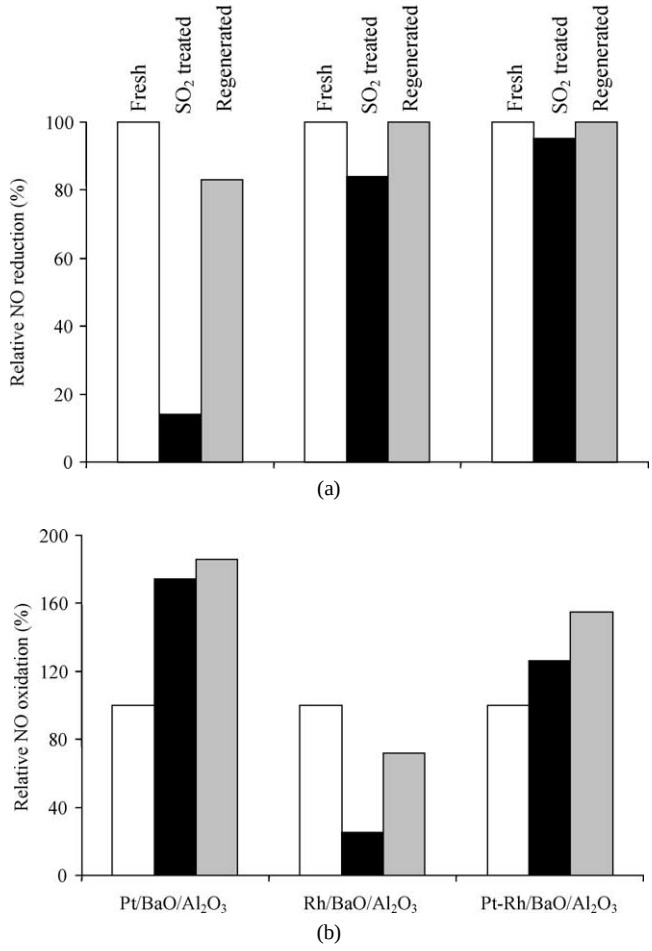

Fig. 10. NO (a) reduction and (b) oxidation activities for BaO/Al_2O_3 catalysts, during rich and lean conditions, with different noble metal compositions (2 wt% Pt, 1 wt% Rh, 2 wt% Pt–1 wt% Rh) as a function of treatment. Lean gas mixture: 8 vol% O_2, 400 vol-ppm NO, 500 vol-ppm C_3H_6, 0 or 25 vol-ppm SO_2. Rich gas mixture: 400 vol-ppm NO, 500 vol-ppm C_3H_6, 0 or 25 vol-ppm SO_2. Temperature: 400 °C. Lean time: 5 min. Rich time: 5 min.

are formed after SO_2 treatment. However, after hydrogen treatment the sulfur signal decreases significantly for the sample containing both Pt and Rh already after 30 min of regeneration in H_2 at 550 °C. After 60 min reduction, the sulfur signal has disappeared. For the sample including only Pt as noble metal, the sulfur signal is only slightly decreased even after 60 min of reduction.

Fig. 10 shows the corresponding activities for NO oxidation during the lean periods and NO reduction during the rich periods after the same treatments as in Fig. 8. An apparent loss of NO reduction activity for $Pt/BaO/Al_2O_3$ is displayed in Fig. 10a. The figure clearly shows that the loss of reduction activity is far more severe for this sample than for the corresponding rhodium-containing samples. Above 80% of the NO reduction activity measured for the fresh catalyst is still available for $Rh/BaO/Al_2O_3$ and Pt–$Rh/BaO/Al_2O_3$ after 150 min of continuous SO_2 exposure. This should be compared with about 15% observed for $Pt/BaO/Al_2O_3$. However, as shown in Fig. 10b, the NO oxidation activity behaves in the opposite way; the oxidation activity of $Rh/BaO/Al_2O_3$ decreases strongly and only 25% of the initial NO oxidation activity remains after sulfur exposure. Moreover, Fig. 10b also shows an increase in NO oxidation activity with sulfur exposure for $Pt/BaO/Al_2O_3$ and Pt–$Rh/BaO/Al_2O_3$.

4. Discussion

This study indicates, as can be seen in Figs. 2–5, that deactivation of the NO_x storage catalysts is much more rapid in the presence of SO_2 under rich than under lean conditions which also is in line with some previous reports [19,23]. The following is often assumed as the mechanism for sulfur deactivation of NO_x storage catalysts: nitrate formation is gradually hindered as more and more of the storage compound becomes stable sulfates [15,17]. Then SO_2 is oxidized to SO_3 and sulfates are formed with the storage compound, e.g., $BaSO_4$ [35]. This may well be an important mechanism for lean conditions. However, it seems to be more important to consider the effect of sulfur

under rich conditions. The findings in this work suggest that interaction of sulfur with the noble metals plays a significant role in this respect.

The noble metals seem to have different roles in the NO_x storage regeneration cycles. Two obvious events on the noble metals are NO oxidation to NO_2, which precedes the storage of NO_x, and reduction of NO to N_2 under rich conditions. All samples investigated show an affected rate of both reactions as a function of the time they have been exposed to SO_2. The effect depends both on the exposure conditions (i.e., SO_2 in lean, rich, or both periods) and the noble metals composition of the catalyst.

Under rich conditions the Rh-containing samples seem to be more resistant to sulfur deactivation regarding NO_x reduction activity (see Fig. 10a) than samples with only Pt as the noble metal. However, with respect to NO oxidation activity the most rapid decrease in activity is observed for samples with only Rh as the noble metal (see Fig. 10b). Pt seems to cause the opposite behavior: a more rapid deactivation of NO_x reduction under rich conditions and a less severe decrease in NO oxidation activity under lean conditions. Actually, an increase is observed for the latter reaction (this is commented on below).

A further indication of the interaction between sulfur and the noble metals is the development of the observed NO desorption peaks. These peaks are of two different natures: The first type, occurring when the conditions are switched from lean to rich, has previously been assigned to NO adsorbed on the noble metals [6] or a need to remove adsorbed oxygen on the noble metal surface before reduction can take place [10,36]. The second type, occurring when the oxygen is turned back on, appears when the samples are exposed to sulfur. This peak has in earlier studies been correlated to blockage of noble metal sites by sulfur species [13,15]. It grows much faster under rich SO_2 exposure than under lean and may therefore be connected to blockage of noble metal sites by reduced sulfur. The sulfur species will prevent NO and O_2 from reaching the noble metal surface and hence inhibit the formation of NO_2, which is crucial to nitrate formation on the storage compound [2–6,12,19, 29,32]. Elementary sulfur deposits have previously been detected on platinum under oxygen deficit [24,25,34] and have been reported to oxidize to SO_2, if exposed to oxygen, with recovered noble metal surface as a consequence [34].

Also, the spectroscopic studies show the interaction of the noble metals with sulfur. The in situ FTIR experiment (Fig. 7) shows that platinum is significantly affected by exposure to sulfur. The disappearance of a CO–Pt peak for the sample that had been exposed to SO_2 under rich conditions shows that the Pt sites become blocked by sulfur [24,25,34,38,39].

The XPS study of the deactivated samples shows formation of sulfates (most likely via SO_3) and formation of Pt and Rh oxides after lean treatments. Platinum sulfate, $Pt(SO_4)_2$ (Pt 4$f_{7/2}$ peak at 74.6 eV [40]), has also been reported to occur [34]. The Pt spectrum after rich SO_2 treatment does not show evidence of sulfate formation. However, the features are relatively broad and we cannot exclude some sulfur deposits on Pt. It should also be noted that the exposure of this sample was not severe (see Experimental Procedure). Further, some sulfur may have transformed to form stable barium sulfates during the time between exposure and analysis. Moreover, both platinum and rhodium sulfides (as well as elementary sulfur) have been detected with this technique previously, both under exposure to SO_2 and H_2S, by Nasri et al. [37] for metals supported on silica. Further, platinum particles deposited on alumina for hydrogenation of aromatics have been reported to form mobile platinum sulfide (PtS) and agglomerates in the presence of H_2S [38]. Sulfur accumulated in barium-based NO_x storage catalysts is known to be released, at least partly, as H_2S during severe hydrogen treatment [14]. It is also well known that H_2S will be formed from SO_2 during rich periods [41]. Additionally, Sedlmair and co-workers [39] recently reported EXAFS observations of PtS species after exposing a $Pt/BaO/Al_2O_3$ type catalyst to a mixture of propene and SO_2. These conditions are similar to those used here, except for the presence of NO.

Oxidation of sulfur deposits may provide an explanation for the fast deactivation of the storage capacity under rich sulfur exposure as follows: Under rich conditions sulfur species, either elementary, sulfidic, or some other kind of reduced sulfur, are adsorbed on the noble metal. When the gas mixture is switched to oxygen excess, these deposits are oxidized, primarily to SO_2, and eventually spill over and form barium sulfates on storage sites close to the noble metals. These sites have previously been acknowledged to be of major importance for NO_x storage [29,42]. Thus, the formation of sulfates at these sites would be expected to significantly affect NO_x storage capacity.

The deactivation of NO_x storage capacity depends not only on the conditions for sulfur exposure but also on the noble metal composition. During SO_2 exposure under rich conditions (Fig. 4), the presence of rhodium in the catalyst decreases deactivation rate compared with platinum only. However, under lean SO_2 exposure the deactivation seems to be independent of the noble metals present in the catalyst. Hence, it may be suggested that the sulfation mechanism by wich the storage sites become trapped as sulfates may dominate under such sulfur exposure.

As mentioned above an increase in the NO oxidation rate is observed after SO_2 exposure for the $Pt/BaO/Al_2O_3$ samples. This behavior has been reported previously by Efthimiadis et al. [43,44] and was assigned to blockage of the NO_x reduction sites on the support (i.e., the NO_2 formed is not reduced and, accordingly, the outlet NO_2 is increased) by Burch and Watling [45]. The present results may be explained by a failure of the samples to be saturated with stored NO_x after 5 min in the fresh state, yielding a too low an initial value to normalize to. Another explanation may be that the formation of platinum oxides is diminished by SO_2, which may reduce the oxides to metallic platinum while forming sulfite and sulfate [46]. The NO/NO_2 equilibrium

over platinum has been reported to be reached faster over the metallic phase compared with the oxides [32]. A third and in our view more likely possibility is sintering of the Pt particles. Is has been shown that larger Pt particles are more effective catalysts for NO oxidation [32] and that Pt sinters under similar conditions [47].

If the sulfur increases the noble metal sintering, not only will the active surface area be decreased (less oxidation and reduction sites) but the NO_x storage function will also be obstructed as the interface between the noble metal and the washcoat, NO_x storage compound included, becomes smaller. This implies that one of the most crucial steps in the NO_x storage mechanism, NO_2 spillover from the noble metal to the storage compound [29,42], may decrease after sulfur exposure.

Also the ability to regenerate the sulfur-deactivated catalysts depends on noble metal composition. In Fig. 10a, it is shown that the NO reduction activity of rhodium under rich conditions is only slightly affected by sulfur treatment. Additionally, the rich sulfur deactivation rate is lower with rhodium present in the catalyst than with platinum solely as indicated in Fig. 4, and as shown in Figs. 8 and 9 the regeneration of rhodium-containing samples is more easily accomplished. It is reasonable to associate these behaviors with rhodium's providing a self-regenerating feature to the catalyst since it is known to be more easily sulfur-regenerated than platinum [37]. Hence, to minimize the effect of sulfur on NO_x storage catalysts, a combination of platinum and rhodium is preferable. This is apparent since the present data (Figs. 8–10) clearly show that such a catalyst is able to retain high NO oxidation activity as well as high NO reduction activity under sulfur exposure and is more easy to regenerate. The regeneration of these types of samples is further examined in a forthcoming publication [48].

5. Conclusions

From the present work it can be concluded that sulfur deactivation of NO_x storage catalysts is strongly dependent on the exposure conditions. Sulfur deactivation occurs when the catalyst is exposed to SO_2 in oxygen excess as well as when the catalyst is exposed to SO_2 under oxygen deficit. The deactivation occurring under rich SO_2 exposure was found to be significantly faster (in time or accumulated dose) than that under lean SO_2 exposure.

The noble metal composition of the catalyst also influenced sulfur deactivation of the catalyst. Lean SO_2 deactivation was found to be independent of noble metal composition of the catalyst, while rich deactivation was found to be slower for samples containing both rhodium and platinum. Additionally, it was established that NO oxidation activity during lean periods and NO_x reduction activity during rich phases were affected differently for rhodium than for platinum. The sample containing only rhodium suffered from severe deactivation of the NO oxidation function under SO_2 exposure but retained good NO_x reduction ability. The opposite behavior was observed for the sample containing only platinum. However, the sample containing both platinum and rhodium maintained NO oxidation activity during the lean periods as well as maintained NO_x reduction activity during the rich periods. Finally, the noble metals present in the catalysts were also determined to affect the sulfur regeneration in hydrogen at 750 °C. The present data showed that recovery of NO_x storage capacity was satisfactory only for samples containing both rhodium and platinum.

Acknowledgments

This work was performed within the Competence Centre for Catalysis hosted by Chalmers University of Technology and financially supported by the Swedish Energy Agency and the member companies AB Volvo, Saab Automobile Powertrain AB, Johnson Matthey CSD, Perstorp AB, Akzo Nobel, MTC AB and the Swedish Space Corporation.

References

[1] P.N. Hawker, Plat. Met. Rev. 39 (1995) 2.
[2] N. Miyoshi, S. Matsamoto, K. Katoh, T. Tanaka, J. Harada, N. Takahashi, K. Yakota, M. Sigiura, K. Kasahara, SAE Tech. Papers Ser. 950809 (1995).
[3] W. Bögner, M. Krämer, B. Kreutzsch, S. Pischinger, D. Voigtländer, G. Wenninger, F. Wirbeleit, M.S. Brogan, R.J. Brisley, D.E. Webster, Appl. Catal. B 7 (1995) 153.
[4] N. Takahashi, H. Shinjoh, T. Iijima, T. Suzuki, K. Yamazaki, K. Yokota, H. Suzuki, N. Miyoshi, S. Matsumoto, T. Tanizawa, T. Tanaka, S. Tateishi, K. Kasahara, Catal. Today 27 (1996) 63.
[5] E. Fridell, M. Skoglundh, S. Johansson, B. Westerberg, A. Törncrona, G. Smedler, Stud. Surf. Sci. Catal. 116 (1998) 537.
[6] E. Fridell, M. Skoglundh, B. Westerberg, S. Johansson, G. Smedler, J. Catal. 183 (1999) 196.
[7] R.J. Ferrauto, R.M. Heck, Catal. Today 51 (1999) 351.
[8] Toyota Jidosha Kabushiki Kaisha, Patent EP 0657 204 A1, 1994.
[9] W.B. Williamson, H.S. Gandhi, P. Wynblatt, T.J. Truex, R.C. Ku, AIChE Symp. Ser. 201 (1980) 212.
[10] I. Nova, L. Castoldi, L. Lietti, E. Tronconi, P. Forzatti, Catal. Today 75 (2002) 431.
[11] N.M.H. Janssen, A.R. Cholach, M. Ikai, K. Tanaka, B.E. Nieuwenhuys, Surf. Sci. 382 (1997) 201.
[12] S. Salasc, M. Skoglundh, E. Fridell, Appl. Catal. B 36 (2002) 145.
[13] P. Engström, A. Amberntsson, M. Skoglundh, E. Fridell, G. Smedler, Appl. Catal. B 22 (1999) L241.
[14] S. Erkfeldt, M. Skoglundh, M. Larsson, Stud. Surf. Sci. Catal. 126 (1999) 211.
[15] A. Amberntsson, B. Westerberg, P. Engström, E. Fridell, M. Skoglundh, Stud. Surf. Sci. Catal. 126 (1999) 317.
[16] H. Mahzoul, L. Limousy, J.F. Brilhac, P. Gilot, J. Anal. Appl. Pyrol. 56 (2000) 179.
[17] T. Asanuma, S. Takeshima, T. Yamashita, T. Tanaka, T. Murai, S. Iguchi, SAE Tech. Paper Ser. 1999-01-3501 (1999).
[18] Sh. Hodjati, F. Semelle, N. Moral, C. Bert, M. Rigaud, SAE Tech. Paper Ser. 2000-01-1874 (2000).
[19] E. Fridell, H. Persson, L. Olsson, B. Westerberg, A. Amberntsson, M. Skoglundh, Top. Catal. 16/17 (2001) 133.
[20] S. Matsumoto, Y. Ikeda, H. Suzuki, M. Ogai, N. Miyoshi, Appl. Catal. B 25 (2000) 115.

[21] I. Hachisuka, H. Hirata, Y. Ikeda, S. Matsumoto, SAE Tech. Paper Ser. 2000-01-1196 (2000).
[22] N. Miyoshi, S. Matsumoto, Stud. Surf. Sci. Catal. 121 (1999) 245.
[23] A. Amberntsson, M. Skoglundh, M. Jonsson, E. Fridell, Catal. Today 73 (2002) 279.
[24] K. Taylor, Catal. Rev. Sci. Eng. 35 (1993) 457.
[25] K. Wilson, C. Hardacre, C.J. Baddeley, J. Lüdecke, D.P. Woodruff, R.M. Lambert, Surf. Sci. 372 (1997) 279.
[26] S. Fendeleur, C. Pope, H. Mahzoul, J.-F. Brilhac, P. Gilot, G. Prado, M. Guyon, B.R. Stanmore, SAE Tech. Paper Ser. 1999-01-3502 (1999).
[27] M. Skoglundh, H. Johansson, L. Löwendahl, K. Jansson, L. Dahl, B. Hirschauer, Appl. Catal. B 7 (1996) 299.
[28] A. Amberntsson, H. Persson, P. Engström, B. Kasemo, Appl. Catal. B 31 (2001) 27.
[29] E. Fridell, H. Persson, B. Westerberg, L. Olsson, M. Skoglundh, Catal. Lett. 66 (2000) 71.
[30] Z. Zsoldos, F. Garin, L. Hilaire, L. Guczi, Catal. Lett. 33 (1995) 39.
[31] J.F. Moulder, W.F. Stickle, P.E. Sobol, K.D. Bomben, in: J. Chastain (Ed.), Handbook of X-ray Photoelectron Spectroscopy, Perkin–Elmer, Physical Electronics Division, Eden Prairie, MN, 1992.
[32] L. Olsson, E. Fridell, J. Catal. 210 (2002) 340.
[33] N. Savargaonkar, B.C. Khanra, M. Pruski, T.S. King, J. Catal. 162 (1996) 277.
[34] T. Wang, A. Vazquez, A. Kato, L.D. Schmidt, J. Catal. 78 (1982) 306.
[35] E. Chaize, D. Webster, B. Krutzsch, G. Wenninger, M. Weibel, Sh. Hodjati, C. Petit, V. Pitchon, A. Kiennemann, R. Loenders, O. Monticelli, P.A. Jacobs, J.A. Martens, B. Kasemo, SAE Tech. Paper Ser. 1998-982593 (1998).
[36] L. Lietti, P. Forzatti, I. Nova, E. Tronconi, J. Catal. 204 (2001) 175.
[37] N.S. Nasri, J.M. Jones, V.A. Dupont, A. Williams, Energy Fuels 12 (1998) 1130.
[38] J.-R. Chang, S.-L. Chang, T.-B. Lin, J. Catal. 169 (1997) 338.
[39] Ch. Sedlmair, K. Seshan, A. Jentys, J.A. Lercher, Catal. Today 75 (2002) 413.
[40] J.S. Hammond, N.J. Winograd, J. Electrochem. Electroanal. Chem. 78 (1977) 55.
[41] R.M. Heck, R.J. Ferrauto, Catalytic Air Pollution Control, Van Nostrand Reinhold, New York, 1995.
[42] L. Olsson, H. Persson, E. Fridell, M. Skoglundh, B. Andersson, J. Phys. Chem. B 105 (2001) 6895.
[43] E.A. Efthimiadis, S.C. Christoforou, A.A. Nikolopoulos, I.A. Vasalos, Appl. Catal. B 22 (1999) 91.
[44] A. Toubeli, E.A. Efthimiadis, I.A. Vasalos, Catal. Lett. 69 (2000) 157.
[45] R. Burch, T.C. Watling, Appl. Catal. B 17 (1998) 131.
[46] A.F. Lee, K. Wilson, R.M. Lambert, C.P. Hubbard, R.G. Hurley, R.W. McCabe, H.S. Gandhi, J. Catal. 184 (1999) 491.
[47] P. Lööf, B. Stenbom, H. Norden, B. Kasemo, J. Catal. 144 (1993) 60.
[48] A. Amberntsson, M. Skoglundh, E. Fridell, manuscript in preparation.